International Journal of Solids and Structures 50 (2013) 3898–3910

Contents lists available at ScienceDirect

International Journal of Solids and Structures

journal homepage: www.elsevier.com/locate/ijsolstr

An embedded crack in a functionally graded orthotropic coating bonded to a homogeneous substrate under a frictional Hertzian contact

Mohamed Ben-Romdhane [a,*], Sami El-Borgi [b,c], Malek Charfeddine [c]

[a] Department of Mathematics and Natural Sciences, Gulf University for Science and Technology, P.O. Box 7207, Hawally 32093, Kuwait
[b] Texas A&M University, Mechanical Engineering Program, Engineering Building, P.O. Box 23874, Education City, Doha, Qatar
[c] Applied Mechanics and Systems Research Laboratory, Tunisia Polytechnic School, University of Carthage, BP 743, 2048 La Marsa, Tunisia

ARTICLE INFO

Article history:
Received 28 February 2013
Received in revised form 20 June 2013
Available online 6 August 2013

Keywords:
Functionally graded orthotropic coating
Stress intensity factor
Singular integral equation
Crack-closure

ABSTRACT

In this paper, we consider the elasto-static problem of an embedded crack in a graded orthotropic coating bonded to a homogeneous substrate subject to statically applied normal and tangential surface loading. The crack direction is parallel to the free surface. The coating is graded in the thickness direction and is orthogonal to the crack direction. This coating is modelled as a non-homogeneous medium with an orthotropic stress–strain law. The equivalent crack surface stresses are first obtained and substituted in the plane elasticity equations. Using integral transforms, the governing equations are converted into singular integral equations which are solved numerically to yield the displacement field as well as the crack-tip stress intensity factors. This study presents a complete theoretical formulation for the problem in the static case. A numerical predictive capability for solving the singular integral equations and computing the crack-tip stress intensity factors is proposed. Since the loading is compressive, a previously developed crack-closure algorithm is applied to avoid interpenetration of the crack faces. The main objective of the paper is to investigate the effects of the material orthotropy and non-homogeneity of the graded coating on the crack-tip stress intensity factors, with and without using the crack-closure algorithm, for the purpose of gaining better understanding on the behavior and design of graded coatings.

1. Introduction

One important challenge in material design is the robustness to cracking and spallation. In fact, layers with different material properties are usually susceptible to cracking, debonding, or spallation because of the discontinuities of their properties along the interface between the materials (Erdogan, 1995). To overcome these drawbacks, an efficient method is to introduce a functionally graded layer with continuous properties at the interface between the coating and the substrate (Li and Guo, 2006). In this manuscript, we focus on the fracture behaviour of graded coatings having properties which vary continuously. Such coatings have the capability to maintaining the structure integrity when subjected to applied mechanical and thermo-mechanical loads (Li and Fan, 2007). Thus, functionally graded materials (FGM) are taking important applications in engineering fields to overcome wear coating and thermal shielding problems such as in cutting tools, high temperature chambers, turbines, micro-electronics and space structures (Holt et al., 1992). They are widely used also as thermal barriers or preventers from chemical corrosion (Li and Fan, 2007).

In spite of the previous advantages of FGM, many tiny defects such as holes and cracks may occur in these materials, due to various causes. Therefore, the study of the fatigue and fracture behaviour of these materials needs a focus on finding solutions to some related crack problems under different loading conditions (Choi, 2004). Actually, one basic problem is to study the stability of these defects, and to investigate their fracture behaviours under different kinds of loads.

Most of the crack problems solved over the past two decades on non-homogeneous materials (Delale and Erdogan, 1983; Dhaliwal and Singh, 1978; Erdogan, 1985; Ozturk and Erdogan, 1993) provide the basis for the fracture mechanics research on FGMs which are essentially non-homogeneous materials. In Erdogan (1995) a brief discussion is given on the application of elementary concepts of fracture mechanics in non-homogeneous materials and a number of typical problem areas are identified which relate to the fracture of FGMs. An important problem is the nature of stress singularities near the tip of a crack embedded in a non-homogeneous medium. Konda and Erdogan (1994) and Jin and Noda (1994) showed that such a crack has the standard square-root singularity in addition to others encountered in a homogeneous medium provided the material property model is continuous and piecewise differentiable.

* Corresponding author. Tel.: +965 25307484; fax: +965 25307030.
E-mail addresses: mbenromd@vt.edu, romdhane.m@gust.edu.kw (M. Ben-Romdhane).

0020-7683/$ - see front matter © 2013 Elsevier Ltd. All rights reserved.
http://dx.doi.org/10.1016/j.ijsolstr.2013.07.025

A number of crack problems in FGMs were solved accounting only for mechanical loading or thermal loading or a combination of both. The crack can be either an internal crack parallel to the free surface or perpendicular to it. Noda and Jin (1993) studied the internal crack problem for an infinite FGM medium subjected to a steady-state heat flux over the crack surfaces by assuming continuously varying thermal properties. The same problem was extended by El-Borgi et al. (2004a) by considering a steady-state heat flux applied away from the crack region, by modeling the crack faces as partially insulated and by accounting for crack-closure effects. The case of an internal fully insulated crack parallel to the boundary of a semi-infinite graded medium subject to a steady-state heat flux applied at the free surface was studied by Jin and Noda (1993). Lee and Erdogan (1998) studied the problem of interface cracking in FGM coatings under steady-state heat flow. Chen and Erdogan (1996) studied the problem of a graded coating on homogeneous substrate with an interface crack subjected to mechanically induced crack surface tractions. El-Borgi et al. (2003, 2004a) extended this problem by considering both thermal and mechanical loads and accounting for crack-closure effects. El-Borgi et al. (2004b) considered the problem of a graded coating bonded to a substrate subjected to a Hertzian contact pressure and with an internal crack embedded in the coating.

Erdogan and Wu (1996) considered a graded strip with a surface crack, perpendicular to the boundaries and parallel to the material gradient, subjected to thermal loads. Later, they solved the same problem by considering mechanical crack surface tractions (Erdogan and Wu, 1997). Dag et al. (1999) and Kadioglu et al. (1998) studied a similar problem with the graded layer attached to an elastic foundation with a crack subjected, respectively, to thermal and mechanical loads. Dag (2001) and Dag and Erdogan (2002)) solved the problem of a surface crack in a graded semi-infinite medium under general loading conditions in which they proposed a method to uncouple the opening and sliding modes. Recently, Gharbi et al. (2009, 2011) studied the elastodynamic problem of a surface crack in a functionally graded coating bonded to a homogeneous substrate under transient thermal loading (Gharbi et al., 2009), as well as under arbitrary dynamic loadings which gives rise to mixed fracture modes (Gharbi et al., 2011).

In all the aforementioned studies, the graded medium is assumed to be isotropic. It is known that because of the processing techniques used in their manufacturing, FGMs are seldom isotropic (Kayserr and Ilsscner, 1995; Sampath et al., 1995). FGMs processed by using a plasma spray technique are known to have a lamellar structure (Sampath et al., 1995). On the other hand, FGMs processed by using the electron beam physical vapor deposition technique generally have a highly columnar structure (Kayserr and Ilsscner, 1995). Thus, in studying fracture mechanics of FGMs, the anisotropic character of these materials has to be taken into account. Instead of using the theory of isotropic elasticity, consideration of an orthotropic elastic non-homogeneous continuum becomes more realistic as far as the modelling of FGMs is considered.

There are few recent studies in the literature dealing with the fracture mechanics of orthotropic FGMs. Among these studies, we can cite the work of Ozturk and Erdogan (1997) who studied the mode I crack problem in an orthotropic graded infinite medium with a crack perpendicular to the material gradient. Later, they extended this problem to the case of a mixed-mode problem in plan elasticity (Ozturk and Erdogan, 1999). Guo et al. (2004) investigated the mode I crack problem in a functionally graded orthotropic strip under static loading. The same problem was studied by Chen et al. (2002) for the case of transient loading. Feng et al. (2003) considered the mode III crack problem in an orthotropic functionally graded strip, and investigated the effects of orthotropy, nonhomogeneity and height of the strip on the energy density factor. Dag et al. (2007, 2008) studied the mixed-mode fracture problem of orthotropic FGM under mechanical and thermal loading conditions. In Dag et al. (2007) the crack was subject to normal and shear tractions applied to its surfaces, the FGM layer had free boundaries. In Dag and Ilhan (2008), the crack was also loaded by self-equilibrating mixed-mode tractions applied to its surfaces and the FGM was bounded to a substrate. In both papers (Dag et al., 2007; Dag and Ilhan, 2008), the analytical solution was based on singular integral equations, the numerical solution was determined using the finite elements method, and the mixed-mode crack-tip parameters were evaluated. Zhou et al. (2007) studied the transient thermal two-dimensional problem of a crack embedded in a graded orthotropic strip, by means of Laplace and Fourier transforms. Later, the same author and collaborators studied again the transient thermal problem of crack in orthotropic FGM, but with the assumption that the orthotropic graded strip is under convective heat supply Zhou et al. (2009). In Zhou et al. (2010), they considered a partially insulated interface crack between a graded orthotropic coating and a homogeneous orthotropic substrate under heat flux supply. Kim and Paulino (2002, 2003, 2004) Kim adopted a finite element methodology for Mode I and mixed-mode fracture analysis of various types of orthotropic FGMs. They evaluated and compared stress intensity factors for mode I and mixed-mode problems by means of the modified crack closure (Kim and Paulino, 2002; Kim and Paulino, 2003). Later, Kim and KC (2008) evaluated T-stress and mixed-mode stress intensity factors under thermo-mechanical loads, by generalizing the interaction integral method. Aoulou et al. (2009) considered the problem of an embedded crack in a graded orthotropic coating bonded to a homogeneous substrate subjected to a compressive loading. The problem was reduced to an eigenvalue problem describing the onset of buckling and the critical buckling strain has been determined.

In the present work, we consider the problem of an orthotropic graded coating bonded to a semi-infinite homogeneous medium with a crack embedded in the FGM layer and parallel to its free surface. The composite medium is subjected to a frictional Hertzian contact traction loading applied to the surface of the graded coating. The applied load is assumed to be a static load. The material properties and elastic stiffness constants in the graded coating are assumed to vary exponentially in the direction perpendicular to the plane of the crack. The crack problem is solved using the method of singular integral equations under the assumption of plane strain or generalized plane stress conditions. However, under certain loading conditions, the mode I stress intensity factor at one or both crack-tips may become negative, which means that the crack faces may come partially or completely in contact. In that case, a crack-closure algorithm developed by El-Borgi et al. (2004a) has been used to compute the contact zone and the correct stress intensity factors assuming frictionless contact between the crack faces. As a first analysis, it is assumed that the crack faces can overlap, and then in the second part of the analysis, the modeling of the crack face contact is accounted for by using a crack-closure algorithm. Our results reflect the effects of the FGM orthotropy and non-homogeneity on the crack-tip stress intensity factors, in order to gain better understanding of the behavior of graded coatings.

2. Problem description and formulation

As shown in Fig. 1, the problem under consideration consists of an infinitely long graded orthotropic coating of thickness $h = h_1 + h_2$, bonded to a homogeneous elastic semi-infinite medium. The graded orthotropic coating contains an embedded crack of length $2a$ along the x-axis and is located at a distance h_1 from the interface and at a depth h_2 from the top surface of the coating. For the graded coating, the material gradient is oriented along the

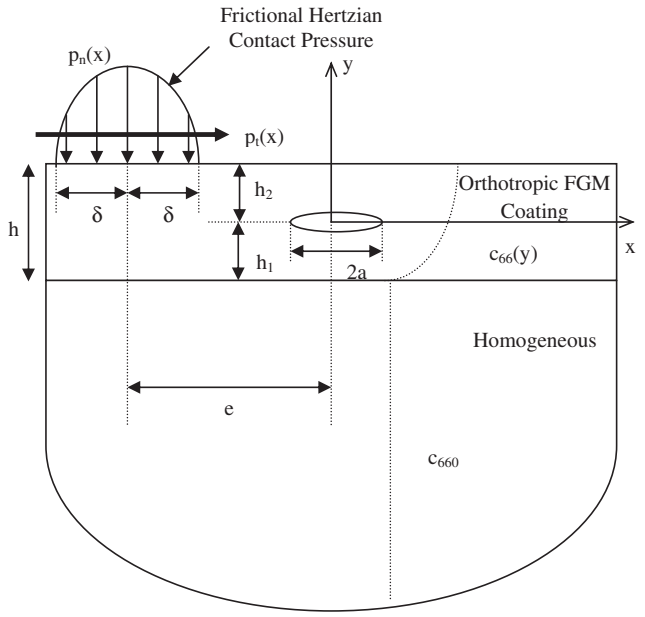

Fig. 1. Geometry and loading of the crack problem.

y-direction. The Poisson's ratio v is assumed to be a constant because the effect of its variation on the crack-tip stress intensity factors was shown to be negligible (Delale and Erdogan, 1983; Erdogan and Wu, 1997) and is equal to the same value as that of the homogeneous substrate.

The other characteristics of the FGM layer are assumed to vary exponentially depending on the y-coordinate. The shear modulus is μ_1, the elastic stiffness constants are c_{11}, c_{22}, c_{12} and c_{66}. They are all modeled, for $-h_1 \leqslant y \leqslant h_2$, by :

$$c_{11} = c_{110}e^{\beta y}, \quad c_{12} = c_{120}e^{\beta y}, \quad c_{22} = c_{220}e^{\beta y}, \quad \mu_1 = c_{66} = c_{660}e^{\beta y}, \tag{1.a-d}$$

where $c_{110}, c_{220}, c_{120}, c_{660}$ are the values of the orthotropic FGM coating properties along the axis $y = 0$ and β is the non-homogeneity parameter controlling their variation in the functionally graded coating. We note that it is for mathematical convenience to assume that all the FGM properties follow the same exponential function.

For the homogeneous elastic substrate, the shear modulus μ_2 is equal to its value at the FGM coating interface, thereby ensuring the continuity of the interface, its value for $y \leqslant -h_1$, is:

$$\mu_2 = c_{660}e^{-\beta h_1}. \tag{1.e}$$

It can be easily shown that the continuity of the mechanical properties between the two media can be imposed only in the shear modulus. It can be shown that attempting to impose the continuity of the others properties leads to a violation of the orthotropic model of the coating.

The coated medium is loaded by a frictional Hertzian contact pressure moving in the $+x$ direction. This type of loading may approximate the distribution of the contact pressure between a rigid inclusion and the layered or graded material (Eberhardt and Kim, 1998; Liu and Chen, 1996; Oliveira and Bower, 1996; Suresh et al., 1997). The normal and the tangential contact tractions are given by the following expressions:

$$p_n(x) = N(x) = p_0\sqrt{1 - \left(\frac{x-e}{\delta}\right)^2}, \quad p_t(x) = T(x) = fp_n(x), \tag{2.a, b}$$

in which p_0 is the peak pressure, e is the location of the contact center, δ is the contact half-width and f is the friction coefficient between the inclusion and the top surface of the FGM layer.

It is noted that the load distribution is derived from a half plane solution. Therefore, the actual distribution of pressure for the contact problem is somewhat different due to the elastic layer effect. A Hertzian distribution is chosen for computational simplicity. A more accurate solution can be obtained using other methods such as in Dag (2001), where the interaction between a rigid indenter and a cracked half space was considered.

The basic equations of the plane problem for non-homogeneous orthotropic elastic solids are the equilibrium equations, the strain–displacement relationships and the linear elastic stress–strain law given respectively by:

$$\frac{\partial\sigma_{xx}}{\partial x} + \frac{\partial\sigma_{xy}}{\partial y} = 0, \quad \frac{\partial\sigma_{xy}}{\partial x} + \frac{\partial\sigma_{yy}}{\partial y} = 0, \tag{3.a, b}$$

$$\varepsilon_{xx} = \frac{\partial u}{\partial x}, \quad \varepsilon_{yy} = \frac{\partial v}{\partial y}, \quad \varepsilon_{xy} = \frac{1}{2}\left(\frac{\partial u}{\partial y} + \frac{\partial v}{\partial x}\right), \tag{4.a-c}$$

$$\sigma_{xx} = c_{11}\frac{\partial u}{\partial x} + c_{12}\frac{\partial v}{\partial y}, \quad -h_1 < y < h_2, \tag{5.a}$$

$$\sigma_{yy} = c_{12}\frac{\partial u}{\partial x} + c_{22}\frac{\partial v}{\partial y}, \quad -h_1 < y < h_2, \tag{5.b}$$

$$\sigma_{xy} = c_{66}\left(\frac{\partial u}{\partial y} + \frac{\partial v}{\partial x}\right), \quad -h_1 < y < h_2, \tag{5.c}$$

For the homogeneous substrate, the linear elastic stress–strain law is given by:

$$\sigma_{xx} = \frac{\mu_2}{\kappa - 1}\left((1+\kappa)\frac{\partial u}{\partial x} + (3-\kappa)\frac{\partial v}{\partial y}\right), \quad y < -h_1, \tag{5.d}$$

$$\sigma_{yy} = \frac{\mu_2}{\kappa - 1}\left((3-\kappa)\frac{\partial u}{\partial x} + (1+\kappa)\frac{\partial v}{\partial y}\right), \quad y < -h_1, \tag{5.e}$$

$$\sigma_{xy} = \mu_2\left(\frac{\partial u}{\partial y} + \frac{\partial v}{\partial x}\right), \quad y < -h_1, \tag{5.f}$$

For the FGM layer, the material properties have the following expressions for plane strain:

$$\kappa = 3 - 4v, \tag{6.a}$$

$$c_{11} = \frac{E_1^2(E_2 - E_3v_{23}^2)}{E_1(E_2 - E_3v_{23}^2) - E_2(E_2v_{12}^2 + E_3v_{13}(v_{13} + 2v_{12}v_{23}))}, \tag{6.b}$$

$$c_{22} = \frac{E_2^2(E_1 - E_3v_{13}^2)}{E_1(E_2 - E_3v_{23}^2) - E_2(E_2v_{12}^2 + E_3v_{13}(v_{13} + 2v_{12}v_{23}))}, \tag{6.c}$$

$$c_{12} = \frac{E_1E_2(E_2v_{12} + E_3v_{13}v_{23})}{E_1(E_2 - E_3v_{23}^2) - E_2(E_2v_{12}^2 + E_3v_{13}(v_{13} + 2v_{12}v_{23}))}, \tag{6.d}$$

$$c_{66} = \mu_1 \tag{6.e}$$

and for generalized plane stress:

$$\kappa = \frac{(3-v)}{(1+v)}, \quad c_{11} = \frac{E_1^2}{E_1 - E_2v_{12}^2}, \quad c_{22} = \frac{E_1E_2}{E_1 - E_2v_{12}^2}, \tag{7.a-c}$$

$$c_{12} = \frac{E_1E_2v_{12}}{E_1 - E_2v_{12}^2}, \quad c_{66} = \mu_1, \tag{7.d, e}$$

where E_1, E_2, E_3 are the elastic moduli in the FGM coating along x, y and $z$axes, respectively, and v_{12}, v_{13}, v_{23} are the Poisson's ratios in planes xy, xz and yz, respectively.

Substituting (4) to (5), inserting the resulting expressions into (3) and using (1) yield the following equations of plane elasticity:

$$c_{110}\frac{\partial^2 u}{\partial x^2}+c_{660}\frac{\partial^2 u}{\partial y^2}+(c_{120}+c_{660})\frac{\partial^2 v}{\partial x\partial y}+\beta c_{660}\left(\frac{\partial u}{\partial y}+\frac{\partial v}{\partial x}\right)=0,\quad -h_1\leqslant y<h_2, \tag{8.a}$$

$$c_{220}\frac{\partial^2 v}{\partial y^2}+c_{660}\frac{\partial^2 v}{\partial x^2}+(c_{120}+c_{660})\frac{\partial^2 u}{\partial x\partial y}+\beta c_{120}\frac{\partial u}{\partial x}+\beta c_{220}\frac{\partial v}{\partial y}=0,\quad -h_1\leqslant y<h_2, \tag{8.b}$$

$$(\kappa+1)\frac{\partial^2 u}{\partial x^2}+(\kappa-1)\frac{\partial^2 u}{\partial y^2}+2\frac{\partial^2 v}{\partial x\partial y}=0,\quad y\leqslant -h_1, \tag{8.c}$$

$$(\kappa+1)\frac{\partial^2 v}{\partial y^2}+(\kappa-1)\frac{\partial^2 v}{\partial x^2}+2\frac{\partial^2 u}{\partial x\partial y}=0,\quad y\leqslant -h_1. \tag{8.d}$$

As shown in Fig. 2, the problem under consideration can be treated as the superposition of two separate problems:

- *Problem 1:* a Neumann boundary value problem which consists of the uncracked coated medium subject to a Hertzian traction loading (Fig. 2(a);
- *Problem 2:* a mixed boundary value problem which consists of the cracked coated medium subject to the equivalent self-equilibrating crack surface stresses $\omega_1(x)$ and $\omega_2(x)$ obtained from the solutions of the previous problem (Fig. 2(b).

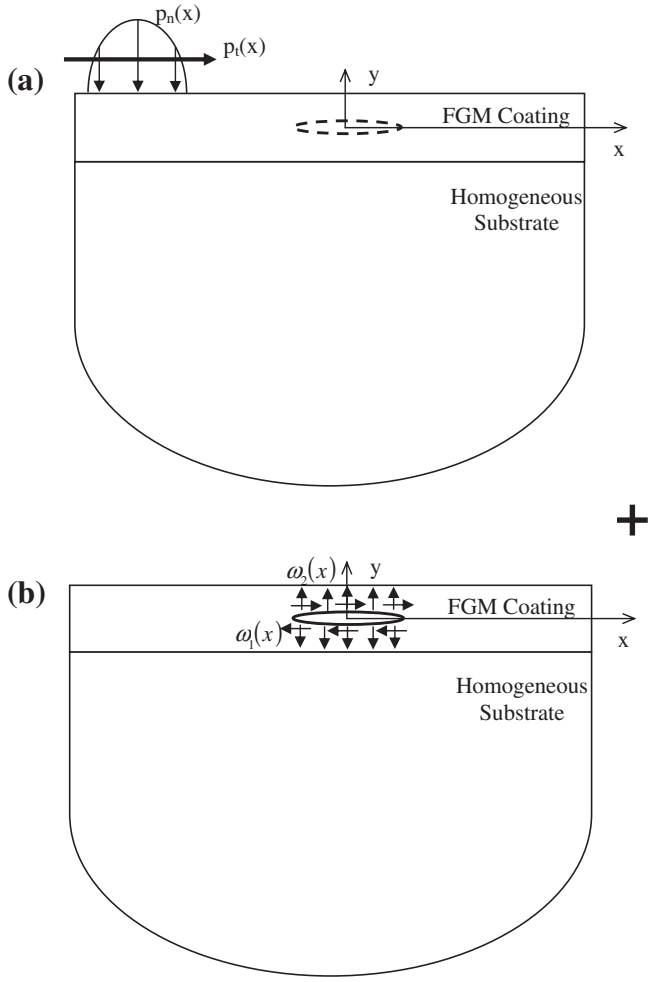

Fig. 2. Superposition of two problems: (a) a Neumann boundary value problem of an uncracked coated medium subject to a Hertzian traction loading; (b) a mixed boundary value problem of a cracked coated medium subject to the equivalent self-equilibrating crack surface stresses obtained from the solution of problem (a).

For problem (1), Eqs. ((8.a)–(8.d)) are subject to the following boundary conditions:

$$\sigma_{xy}(x,h_2)=p_t(x),\quad |x-e|\leqslant\delta, \tag{9.a}$$

$$\sigma_{xy}(x,h_2)=0,\quad |x-e|>\delta, \tag{9.b}$$

$$\sigma_{yy}(x,h_2)=-p_n(x),\quad |x-e|\leqslant\delta, \tag{10.a}$$

$$\sigma_{yy}(x,h_2)=0,\quad |x-e|>\delta, \tag{10.b}$$

$$\sigma_{xy}(x,-h_1^+)=\sigma_{xy}(x,-h_1^-),\quad |x|<+\infty, \tag{11.a}$$

$$\sigma_{yy}(x,-h_1^+)=\sigma_{yy}(x,-h_1^-),\quad |x|<+\infty, \tag{11.b}$$

$$u(x,-h_1^+)=u(x,-h_1^-),\quad |x|<+\infty. \tag{12.a}$$

$$v(x,-h_1^+)=v(x,-h_1^-),\quad |x|<+\infty. \tag{12.b}$$

$$\sigma_{xy}(x,y)=\sigma_{yy}(x,y)=0,\quad |y|\to+\infty,\quad |x|<+\infty. \tag{13.a, b}$$

Eqs. (9.a) and (10.a) correspond to the Hertzian distribution of the contact pressure between the inclusion and the graded coating. Eqs. (9.b) and (10.b) indicate that no tractions are applied at the top surface of the FGM coating outside the contact region. Eqs. (11.a)–(12.b) describe the continuity conditions of the stress and displacement fields along the interface $y=-h_1$. Eqs. (13.a) and (13.b) indicate that stresses vanish at $y\to-\infty$;.

For problem (2), Eqs. (8.a)–(8.d) are subject to the following boundary conditions:

$$\sigma_{xy}(x,0^+)=\sigma_{xy}(x,0^-)=\omega_1(x),\quad |x|\leqslant a, \tag{14}$$

$$\sigma_{yy}(x,0^+)=\sigma_{yy}(x,0^-)=\omega_2(x),\quad |x|\leqslant a, \tag{15}$$

$$\sigma_{xy}(x,0^+)=\sigma_{xy}(x,0^-)=0,\quad |x|>a, \tag{16.a}$$

$$\sigma_{yy}(x,0^+)=\sigma_{yy}(x,0^-)=0,\quad |x|>a, \tag{16.b}$$

$$u(x,0^+)=u(x,0^-)=0,\quad |x|>a, \tag{17.a, b}$$

$$v(x,0^+)=v(x,0^-)=0,\quad |x|>a, \tag{17.c, d}$$

$$\sigma_{xy}(x,-h_1^+)=\sigma_{xy}(x,-h_1^-),\quad |x|<+\infty, \tag{18.a}$$

$$\sigma_{yy}(x,-h_1^+)=\sigma_{yy}(x,-h_1^-),\quad |x|<+\infty, \tag{18.b}$$

$$u(x,-h_1^+)=u(x,-h_1^-),\quad |x|<+\infty. \tag{18.c}$$

$$v(x,-h_1^+)=v(x,-h_1^-),\quad |x|<+\infty. \tag{18.d}$$

$$\sigma_{xy}(x,h_2)=\sigma_{yy}(x,h_2)=0,\quad |x|<+\infty \tag{19.a, b}$$

$$\sigma_{xy}(x,y)=\sigma_{yy}(x,y)=0,\quad y\to-\infty,\quad |x|<+\infty \tag{20.a, b}$$

Eqs. (14) and (15) describe, respectively, the applied tangential and normal crack surface tractions which can be expressed in terms of the Hertzian contact loading based on the resolution of problem (1). Eqs. (16.a)–(18.d) describe the continuity conditions of the stress and displacement fields along, respectively, the crack axis and outside the crack $y=0$ and along the interface $y=-h_1$.

Eq. (19) indicates that no tractions are applied at the top surface of the graded coating while Eq. (20) indicates that stresses vanish at $y\to-\infty$ and hence represent the regularity conditions at $y\to-\infty$.

We now define the following dimensionless quantities:

$$\bar{\sigma}_{xy} = \frac{\sigma_{xy}}{c_{660}}, \quad \bar{\sigma}_{yy} = \frac{\sigma_{yy}}{c_{660}}, \tag{21.a-b}$$

$$(\bar{x}, \bar{y}) = \frac{(x, y)}{a}, \quad (\bar{u}, \bar{v}) = \frac{(u, v)}{a}, \tag{21.c-f}$$

$$\bar{\beta} = \beta a, \tag{21.g}$$

For simplicity of notation, in what follows, the bar appearing with the dimensionless quantities is omitted.

3. Equivalent crack surface stresses

The solution of problem (1) is briefly summarized in Appendix A. The expressions of the equivalent self equilibrating tangential and normal crack surface stresses, which are obtained from Equations (A.11) and (A.12) by setting $\tilde{y} = 0$ and $|x| \leqslant 1$ corresponding to the crack location, are, respectively given by :

$$\omega_1(x) = \frac{e^{\beta(\tilde{y}-h)}}{2\pi} \int_{e-\delta}^{e+\delta} \int_{-\infty}^{+\infty} \left(\sum_{j=1}^{4} (-1)^{j+1} \frac{\tilde{D}_{1j}}{\tilde{D}} \tilde{q}_j e^{m_j \tilde{y}} \right) p_t(t) e^{i\alpha(t-x)} d\alpha dt - \frac{e^{\beta(\tilde{y}-h)}}{2\pi} \int_{e-\delta}^{e+\delta} \int_{-\infty}^{+\infty} \left(\sum_{j=1}^{4} (-1)^{k} \frac{\tilde{D}_{2j}}{\tilde{D}} \tilde{q}_j e^{m_j \tilde{y}} \right) (\kappa - 1) p_n(t) e^{i\alpha(t-x)} d\alpha dt \tag{22.a}$$

$$\omega_2(x) = \frac{e^{\beta(\tilde{y}-h)}}{2\pi(\kappa-1)} \int_{e-\delta}^{e+\delta} \int_{-\infty}^{+\infty} \left(\sum_{j=1}^{4} (-1)^{j+1} \frac{\tilde{D}_{1j}}{\tilde{D}} \tilde{p}_j e^{m_j \tilde{y}} \right) p_t(t) e^{i\alpha(t-x)} d\alpha dt - \frac{e^{\beta(\tilde{y}-h)}}{2\pi} \int_{e-\delta}^{e+\delta} \int_{-\infty}^{+\infty} \left(\sum_{j=1}^{4} (-1)^{j} \frac{\tilde{D}_{2j}}{\tilde{D}} \tilde{p}_j e^{m_j \tilde{y}} \right) p_n(t) e^{i\alpha(t-x)} d\alpha dt \tag{22.b}$$

4. Displacement field in cracked medium

For problem (2) the plane elasticity Eqs. (8.a)–(8.d) are solved using standard Fourier transforms to yield the displacement field in the graded coating and in the homogeneous substrate which, after applying the regularity condition (20), is expressed as follows:

$$u(x,y) = \int_{-\infty}^{+\infty} \left(\sum_{j=1}^{4} C_j(\alpha) e^{m_j y} \right) e^{-ix\alpha} d\alpha, \quad 0 < y \leqslant h_2, \tag{23.a}$$

$$v(x,y) = \int_{-\infty}^{+\infty} \left(\sum_{k=1}^{4} C_j(\alpha) s_j(\alpha) e^{m_j y} \right) e^{-ix\alpha} d\alpha, \quad 0 < y \leqslant h_2, \tag{23.b}$$

$$u(x,y) = \int_{-\infty}^{+\infty} \left(\sum_{j=1}^{4} C_{j+4}(\alpha) e^{m_j y} \right) e^{-ix\alpha} d\alpha, \quad -h_1 \leqslant y < 0, \tag{23.c}$$

$$v(x,y) = \int_{-\infty}^{+\infty} \left(\sum_{k=1}^{4} C_{j+4}(\alpha) s_j(\alpha) e^{m_j y} \right) e^{-ix\alpha} d\alpha, \quad -h_1 \leqslant y < 0, \tag{23.d}$$

$$u(x,y) = \int_{-\infty}^{+\infty} (C_5(\alpha) + C_6(\alpha) y) e^{|\alpha| y} e^{-ix\alpha} d\alpha, \quad y \leqslant -h_1, \tag{23.e}$$

$$v(x,y) = \int_{-\infty}^{+\infty} [C_5(\alpha) s_5 + C_6(\alpha)(y s_5 + s_6)] e^{|\alpha| y} e^{-ix\alpha} d\alpha, \quad y \leqslant -h_1, \tag{23.f}$$

where $C_k(\lambda)$ $(k = 1, \ldots, 10)$ are unknown functions determined from the boundary conditions, and $m_1, \ldots, m_4$ are the roots of the characteristic polynomial associated with the plane elasticity Eqs. (8.a) and (8.b) which are given by:

$$\begin{aligned} m_1 &= \tfrac{1}{2}\left(-\beta + \sqrt{\beta^2 + 4\kappa_0\alpha^2 + 4\alpha\sqrt{\alpha^2(\kappa_0^2 - \delta_0) - \beta^2 v_0}} \right) \\ m_2 &= \tfrac{1}{2}\left(-\beta - \sqrt{\beta^2 + 4\kappa_0\alpha^2 + 4\alpha\sqrt{\alpha^2(\kappa_0^2 - \delta_0) - \beta^2 v_0}} \right) \\ m_3 &= \tfrac{1}{2}\left(-\beta + \sqrt{\beta^2 + 4\kappa_0\alpha^2 - 4\alpha\sqrt{\alpha^2(\kappa_0^2 - \delta_0) - \beta^2 v_0}} \right) \\ m_4 &= \tfrac{1}{2}\left(-\beta - \sqrt{\beta^2 + 4\kappa_0\alpha^2 - 4\alpha\sqrt{\alpha^2(\kappa_0^2 - \delta_0) - \beta^2 v_0}} \right) \end{aligned} \quad -h_1 < y < h_2, \tag{24.a-d}$$

$$\begin{aligned} n_{1,2} &= \alpha \\ n_{3,4} &= -\alpha \end{aligned} \quad y \leqslant -h_1, \tag{24.e-h}$$

in which:

$$\kappa_0 = \frac{c_{110}c_{220} - 2c_{120}c_{660} - c_{120}^2}{2c_{660}c_{220}}, \quad \delta_0 = \frac{c_{110}}{c_{220}}, \quad v_0 = \frac{c_{120}}{c_{220}}, \tag{25.a-c}$$

and where $s_1, \ldots, s_6$ are determined by substituting (23.a) to (23.f) to (8.a-d) as follows:

$$s_k = \frac{c_{660} m_k (m_k + \beta) - c_{110}\alpha^2}{i\alpha((c_{120} + c_{660}) m_k + \beta c_{660})} \quad (k = 1, \ldots, 4), \tag{26.a}$$

$$s_5 = \frac{i\alpha}{|\alpha|}, \quad s_6 = -\frac{i\kappa}{\alpha}. \tag{26.b, c}$$

For this mixed-boundary value problem (*i.e.* problem (2)), the main unknowns of interest are the so-called density functions chosen for convenience as the derivatives of the relative crack opening displacements. These density functions are given by:

$$\psi_1(x) = \frac{\partial}{\partial x}\left[u(x,0^+) - u(x,0^-)\right], \quad \psi_2(x) = \frac{\partial}{\partial x}\left[v(x,0^+) - v(x,0^-)\right], \tag{27.a, b}$$

which satisfy the following single-valuedness conditions:

$$\int_{-a}^{+a} \psi_j(t) dt = 0 \quad (j = 1, 2), \quad \psi_j(x) = 0 \quad (j = 1, 2) \quad |x| \geqslant a. \tag{28.a, b}$$

Applying the boundary conditions (16) to (19) , we obtain a linear algebraic system of equations in which the unknown functions $C_k(\alpha)(k = 1, \ldots, 10)$ are expressed in terms of the unknown density functions ψ_1 and ψ_2 as follows:

$$\sum_{j=1}^{4} q_j e^{m_j h_2} C_j = 0, \quad \sum_{j=1}^{4} p_j e^{m_j h_2} C_j = 0, \tag{29.a, b}$$

$$\sum_{j=1}^{4} q_j C_j - \sum_{j=1}^{4} q_j C_{j+4} = 0, \quad \sum_{j=1}^{4} p_j C_j - \sum_{j=1}^{4} p_j C_{j+4} = 0, \tag{29.c, d}$$

$$\sum_{j=1}^{4} q_j e^{-m_j h_1} C_{j+4} - q_5 e^{-|\alpha| h_1} C_9 - q_6 e^{-|\alpha| h_1} C_{10} = 0, \tag{29.e}$$

$$\sum_{j=1}^{4} p_j e^{-m_j h_1} C_{j+4} - p_5 e^{-|\alpha| h_1} C_9 - p_6 e^{-|\alpha| h_1} C_{10} = 0, \tag{29.f}$$

$$\sum_{j=1}^{4} e^{-m_j h_1} C_{j+4} - e^{-|\alpha| h_1} C_9 + h_1 e^{-|\alpha| h_1} C_{10} = 0, \tag{29.g}$$

$$\sum_{j=1}^{4} s_j e^{-m_j h_1} C_{j+4} - s_5 e^{-|\alpha| h_1} C_9 - (s_6 - h_1 s_5) e^{-|\alpha| h_1} C_{10} = 0, \tag{29.h}$$

$$\sum_{j=1}^{4} C_j - \sum_{j=1}^{4} C_{j+4} = F_1(\alpha), \quad \sum_{j=1}^{4} C_j s_j - \sum_{j=1}^{4} C_{j+4} s_j = F_2(\alpha), \tag{29.i,j}$$

where

$$F_j(\alpha) = \frac{i}{2\pi\alpha} \int_{-1}^{+1} \psi_j(t) e^{it\alpha} dt \quad (j = 1, 2), \tag{30.a, b}$$

and where: p_j and $q_j (j = 1 \ldots 4)$, are the quantities expressed in Appendix B.

From the linear algebraic system already determined, the functions $C_j(\alpha)(j = 1, \ldots, 10)$ can be expressed in terms of the unknown density functions ψ_1 and ψ_2.

Applying the remaining boundary conditions (14) and (15) yields the following coupled singular integral equations in which the unknowns are the density functions ψ_1 and ψ_2 and which after extracting the Cauchy singularity from the kernels take the following form:

$$\int_{-1}^{+1} \left[\left(\frac{1}{t-x} + k_{11}(x,t) \right) \psi_1(t) + k_{12}(x,t) \psi_2(t) \right] dt = \frac{\pi\sqrt{2}\sqrt{\kappa_0 + \sqrt{\delta_0}}}{(\kappa_0 + \upsilon_0)} \omega_1(x), \quad |x| \leqslant 1, \tag{31.a}$$

$$\int_{-1}^{+1} \left[k_{21}(x,t) \psi_1(t) + \left(\frac{1}{t-x} + k_{22}(x,t) \right) \psi_2(t) \right] dt = \frac{\pi\sqrt{2\delta_0}\sqrt{\kappa_0 + \sqrt{\delta_0}}}{(\kappa_0 + \upsilon_0)} \omega_2(x), \quad |x| \leqslant 1, \tag{31.b}$$

where the known functions $k_{11}(x,t), k_{12}(x,t), k_{21}(x,t)$ and $k_{22}(x,t)$ are Fredholm kernels that depend on the non-homogeneity parameter β which expressions are given in Appendix B.

It was shown by Erdogan et al. (1973) that the solution of (31.a,b) subject to the single-valuedness condition (28) can be expressed as $\psi_i(t) = w(t)\phi_i(t)(i = 1, 2)$ where $w(t) = 1/\sqrt{1-t^2}$ is the weight function associated with the Chebyshev polynomial of the first kind $T_n(t) = \cos(n \arccos(t))$ and $\phi_i(t)$ is a continuous and bounded function in the interval $[-1 \quad 1]$ which can be expressed as a truncated series of Chebyshev polynomial of the first kind. Therefore, the solution of (30.a,b) may be expressed as

$$\psi_1(t) = \sum_{n=1}^{N} \tilde{a}_n T_n(t) \Big/ \sqrt{1-t^2}, \quad \psi_2(t) = \sum_{n=1}^{N} \tilde{b}_n T_n(t) \Big/ \sqrt{1-t^2}. \tag{32.a, b}$$

Substituting (32) to (31) yields two linear algebraic equations for the $2N$ unknowns $\tilde{a}_n, \tilde{b}_n (n = 1, \ldots, N)$. Furthermore, discretizing the spatial variable x using a suitable collocation method, such as the one given below

$$x_j = \cos\left[\frac{(2j-1)\pi}{2N} \right], \quad (j = 1, \ldots, N), \tag{33}$$

yields a system of $2N$ linear algebraic equations in terms of the $2N$ unknowns $\tilde{a}_n$, $\tilde{b}_n$ $(n = 1, \ldots, N)$.

Once the coefficients $\tilde{a}_n$ and $\tilde{b}_n (n = 1, \ldots, N)$ are determined, the functions $C_k(\alpha)(\mathrm{k} = 1, \ldots, 10)$ can be then computed, which leads to the x and y components of the displacement and stress fields in the composite medium.

5. Stress intensity factors

The stress intensity factors at both crack-tips can be determined from the expressions of the stress field as follows (El-Borgi et al., 2004a,b):

$$k_1(1) = \lim_{x \to 1} \sqrt{2(x-1)} \sigma_{yy}(x, 0), \quad k_1(-1) = \lim_{x \to -1} \sqrt{2(-x-1)} \sigma_{yy}(x, 0), \tag{34.a, b}$$

$$k_2(1) = \lim_{x \to 1} \sqrt{2(x-1)} \sigma_{xy}(x, 0), \quad k_2(-1) = \lim_{x \to -1} \sqrt{2(-x-1)} \sigma_{xy}(x, 0), \tag{34.c, d}$$

which can be expressed in terms of the unknown coefficients $\tilde{a}_n$ and $\tilde{b}_n, (n = 1, \ldots, N)$ related, respectively, to the density functions ψ_1 and ψ_2 (Eqs. (19.a) and (19.b)), as follows:

$$k_1(1) = \frac{-(\kappa_0 + \upsilon_0)}{\sqrt{2}\sqrt{\delta_0}\sqrt{\kappa_0 + \sqrt{\delta_0}}} \sum_{n=1}^{N} \tilde{b}_n, \tag{35.a}$$

$$k_1(-1) = \frac{(\kappa_0 + \upsilon_0)}{\sqrt{2}\sqrt{\delta_0}\sqrt{\kappa_0 + \sqrt{\delta_0}}} \sum_{n=1}^{N} (-1)^n \tilde{b}_n, \tag{35.b}$$

$$k_2(1) = \frac{-(\kappa_0 + \upsilon_0)}{\sqrt{2}\sqrt{\kappa_0 + \sqrt{\delta_0}}} \sum_{n=1}^{N} \tilde{a}_n, \tag{35.c}$$

$$k_2(-1) = \frac{(\kappa_0 + \upsilon_0)}{\sqrt{2}\sqrt{\kappa_0 + \sqrt{\delta_0}}} \sum_{n=1}^{N} (-1)^n \tilde{a}_n. \tag{35.d}$$

6. Crack-closure algorithm

In some cases, mode I Stress Intensity Factor may become negative at one or both crack-tips, which means that the crack faces become in contact over a certain part or over the entire crack length. In that case, a crack closure algorithm should be applied.

Table 1
Crack closure configurations for which the mode I stress intensity factor is negative at one or both crack-tips (El-Borgi et al., 2004a).

Case No.	Crack-contact configuration	Sign of $k_1(-1)$ and $k_1(+1)$	Crack closure algorithm	
			Assume	Until
1	-1 c Crack +1, b^l	$k_1(-1) < 0$, $k_1(+1) > 0$	b^l	$k_1(-1 + b^l) = 0$
2	-1 Crack d +1, b^r	$k_1(-1) > 0$, $k_1(+1) < 0$	b^r	$k_1(1 - b^r) = 0$
3	-1 c Crack d +1, b^l b^r	$k_1(-1) < 0$, $k_1(+1) < 0$	b^l and b^r	$k_1(-1 + b^l) = 0$, and $k_1(1 - b^r) = 0$

Table 2
Mechanical properties of the orthotropic functionally graded materials used in the analysis.

	c_{110}	c_{120}	c_{220}	c_{660}
FGM I	1.578×10^{10}	3.248×10^{9}	1.048×10^{10}	7.070×10^{9}
FGM II	1.048×10^{10}	3.248×10^{9}	1.578×10^{10}	7.070×10^{9}

In the present work, a crack closure algorithm developed by El-Borgi et al. (2004a), which is described in following paragraph- is used. Table 1 shows the three possible crack-closure configurations for which the mode I stress intensity factor is negative at one or at both crack-tips:

- In case 1, k_1(-1) is negative and k_1(+1) is positive which means that the crack is opened at its right tip (x = 1), and is closed at its left tip (x = -1), over a length denoted b^l. The value of b^l is determined from the condition k_1 (-1+b^l) = 0 which can be solved using a linear interpolation method.
- In case 2, k_1 (+1) is negative and k_1 (-1) is positive which means that the crack is opened at its left tip (x = -1), and is closed at its right tip (x= 1), over a length denoted b^r. The value of b^r is determined from the condition k_1 (1-b^r) = 0.
- In case 3, k_1 (+1) and k_1 (-1) are negative which means that the crack is closed at its both tips, over lengths denoted b^r from the right and b^l from the left. Their values are determined from the conditions k_1 (1-b^r) = 0 and k_1 (-1+b^l) = 0.

Taking in consideration these conditions, Eqs. (31.a) and (31.b) become:

$$\int_{-1}^{+1}\left[\left(\frac{1}{t-x}+k_{11}(x,t)\right)\psi_1(t)\right]dt+\int_c^d [k_{12}(x,t)\psi_2(t)]dt = \frac{\pi\sqrt{2}\sqrt{\kappa_0+\sqrt{\delta_0}}}{(\kappa_0+\upsilon_0)}\omega_1(x), \quad |x|\leqslant 1, \tag{36.a}$$

$$\int_{-1}^{+1} k_{21}(x,t)\psi_1(t)dt+\int_c^d\left(\frac{1}{t-x}+k_{22}(x,t)\right)\psi_2(t)dt = \frac{\pi\sqrt{2\delta_0}\sqrt{\kappa_0+\sqrt{\delta_0}}}{(\kappa_0+\upsilon_0)}\omega_2(x), \quad |x|\leqslant 1, \tag{36.b}$$

in which $c = -1 + b^l$, and $d = 1 - b^r$.

We apply the following normalizations and definitions:

$$x=\frac{1}{2}(d-c)r+\frac{1}{2}(d+c), \quad t=\frac{1}{2}(d-c)s+\frac{1}{2}(d+c), \tag{37.a, b}$$

$$\omega_2(x)=\tilde{\omega}_2(r), \quad \psi_2(t)=\tilde{\psi}_2(s), \tag{37.c, d}$$

$$k_{21}(x,t)=\tilde{k}_{21}(x,s), \quad k_{21}(x,t)=\tilde{k}_{21}(r,t), \tag{37.e, f}$$

$$k_{22}(x,t)=\tilde{k}_{22}(r,t), \tag{37.g}$$

Eqs. (36.a) and (36.b):

$$\int_{-1}^{+1}\left[\left(\frac{1}{t-x}+k_{11}(x,t)\right)\psi_1(t)\right]dt+\int_{-1}^{1}\frac{d-c}{2}\tilde{k}_{12}(x,s)\tilde{\psi}_2(s)ds = \frac{\pi\sqrt{2}\sqrt{\kappa_0+\sqrt{\delta_0}}}{(\kappa_0+\upsilon_0)}\omega_1(x), \quad |x|\leqslant 1, \tag{38.a}$$

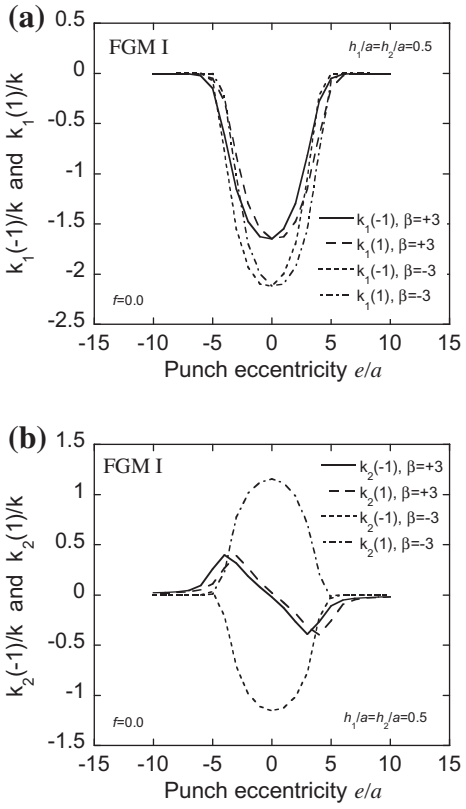

Fig. 3. Normalized mode I and II stress intensity factors $(k_1, k_2)/k$ variation with the punch eccentricity, using the Orthotropic FGM I properties, for the case of a compliant coating $\beta a = -3$ and stiff coating $\beta a = 3$ and no friction, $f = 0$; disregarding crack-closure, $k = p_0\sqrt{a}$, and for $\nu = 0.3$, $\delta = 4a$, $h_1 = h_2 = 0.5a$.

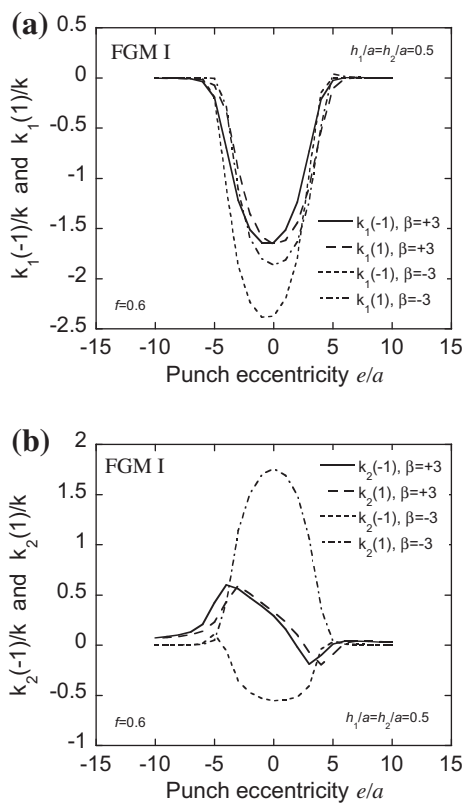

Fig. 4. Normalized mode I and II stress intensity factors $(k_1, k_2)/k$ variation with the punch eccentricity, using the Orthotropic FGM I properties, for the case of a compliant coating $\beta a = -3$ and stiff coating $\beta a = 3$ and dry friction, $f = 0.6$; disregarding crack-closure, $k = p_0\sqrt{a}$, and for $\nu = 0.3$, $\delta = 4a$, $h_1 = h_2 = 0.5a$.

$$\int_{-1}^{+1}\tilde{k}_{21}(r,t)\psi_1(t)dt+\int_{-1}^{1}\left(\frac{1}{s-r}+\frac{d-c}{2}\tilde{k}_{22}(r,s)\right)\tilde{\psi}_2(s)ds = \frac{\pi\sqrt{2\delta_0}\sqrt{\kappa_0+\sqrt{\delta_0}}}{(\kappa_0+\upsilon_0)}\tilde{\omega}_2(r), \quad |r|\leqslant 1, \tag{38.b}$$

And the expressions of the SIFs become:

$$k_1(d)=\frac{-(\kappa_0+\upsilon_0)}{\sqrt{2}\sqrt{\delta_0}\sqrt{\kappa_0+\sqrt{\delta_0}}}\sqrt{\frac{d-c}{2}}\sum_{n=1}^{N}\tilde{b}_n, \tag{39.a}$$

$$k_1(c)=\frac{(\kappa_0+\upsilon_0)}{\sqrt{2}\sqrt{\delta_0}\sqrt{\kappa_0+\sqrt{\delta_0}}}\sqrt{\frac{d-c}{2}}\sum_{n=1}^{N}(-1)^n\tilde{b}_n, \tag{39.b}$$

$$k_2(d)=\frac{-(\kappa_0+\upsilon_0)}{\sqrt{2}\sqrt{\kappa_0+\sqrt{\delta_0}}}\sum_{n=1}^{N}\tilde{a}_n, \tag{39.c}$$

$$k_2(c)=\frac{(\kappa_0+\upsilon_0)}{\sqrt{2}\sqrt{\kappa_0+\sqrt{\delta_0}}}\sum_{n=1}^{N}(-1)^n\tilde{a}_n. \tag{39.d}$$

7. Results and discussion

The geometry and coordinate system of the considered problem is shown in Fig. 1. The compressive contact and presence of an embedded crack parallel to the free surface of the graded coating will produce a state of interpenetration unless a crack-closure algorithm is established as discussed earlier. Thus, we consider two cases:

(1) the case when interpenetration is allowed ;
(2) a crack-closure algorithm (described in Section 6) is invoked.

Numerical calculations are carried out for two kinds of material properties (Orthotropic FGM I and Orthotropic FGM II), whose mechanical properties are listed in Table 2. The only difference between the two orthotropic materials is that their reinforced directions are perpendicular to each other. On the other hand, we consider two cases of FGM materials, a compliant coating ($\beta a=-3$), and a stiff coating ($\beta a=+3$). The coatings will have a thickness h, and the contact length is $\delta=4a$. The crack is located in the interval $[-a,a]$.

Fig. 3 illustrates the effect of the punch eccentricity on the mode I and II crack-tip stress intensity factors (SIF) on left and on the right tip of the crack for the first kind material properties (Orthotropic FGM I). The results were calculated for plane strain conditions, $\nu=0.3, h_1/a=h_2/a=0.5$, no friction $f=0$, and for two values of the non-homogeneity parameter β controlling the variation of the material properties of the FGM coating $\beta a=3$ and $\beta a=-3$.

The Fig. 3 shows that interpenetration of the crack surfaces has occurred because the SIFs of the mode I have negative values. Although this case is not physically admissible unless the normal load is reversed, the figure can be used to study the difference between the results for stiff and compliant FGMs. The results show that for the mode I SIF, there is a little difference between the two cases of stiff and compliant FGMs. However, for the mode II SIF, there is a considerable difference between compliant FGMs and stiff FGMs. In addition, the sign of the punch eccentricity influences the stability of the crack. With a compliant coating ($\beta a=-3$), a symmetric distribution of $k_2(-1)$ and $k_2(+1)$, while a

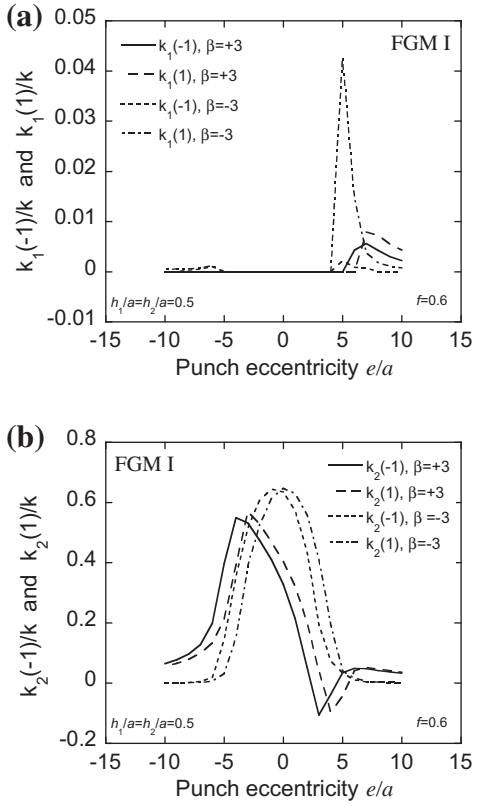

Fig. 5. Crack-closure computed Normalized mode I and II stress intensity factors $(k_1,k_2)/k$ variation with the punch eccentricity, using the Orthotropic FGM I properties, for the case of a compliant coating $\beta a=-3$ and stiff coating $\beta a=3$ and dry friction, $f=0.6$; $k=p_0\sqrt{a}$, and for $\nu=0.3$, $\delta=4a, h_1=h_2=0.5a$.

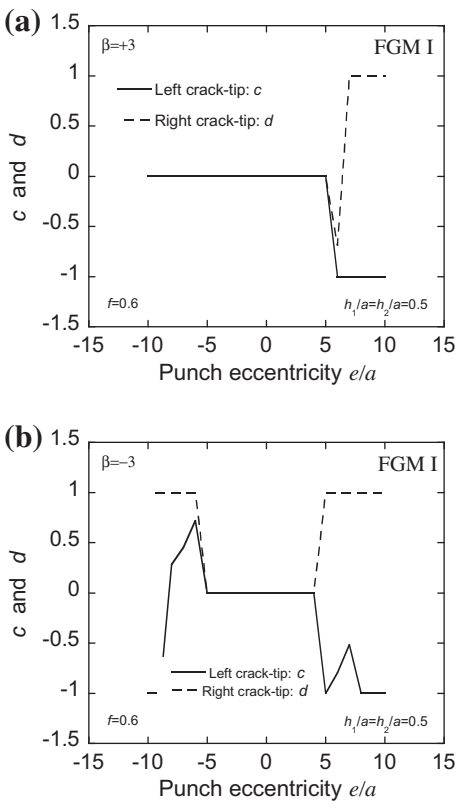

Fig. 6. Normalized crack length (left and right crack-tip) variation with the punch eccentricity, using the Orthotropic FGM I properties, for the case of a compliant coating $\beta a=-3$ and stiff coating $\beta a=3$ and dry friction, $f=0.6$; and for $\nu=0.3$, $\delta=4a, h_1=h_2=0.5a$.

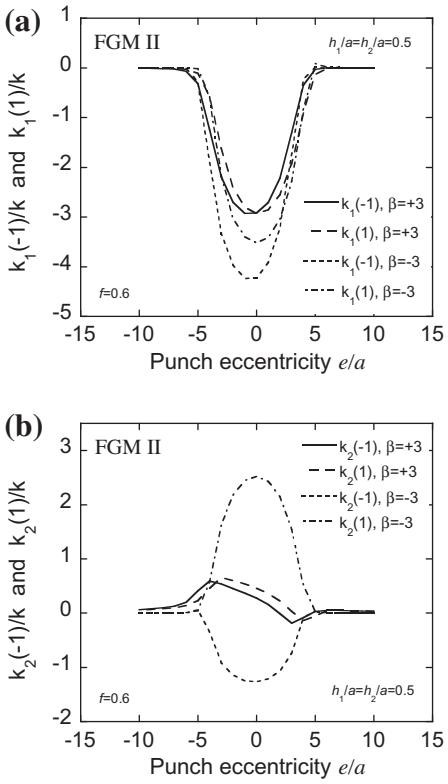

Fig. 7. Normalized mode I and II stress intensity factors $(k_1, k_2)/k$ variation with the punch eccentricity, using the Orthotropic FGM II properties, for the case of a compliant coating $\beta a = -3$ and stiff coating $\beta a = 3$ and dry friction, $f = 0.6$; disregarding crack-closure, $k = p_0\sqrt{a}$, and for $\nu = 0.3$, $\delta = 4a, h_1 = h_2 = 0.5a$.

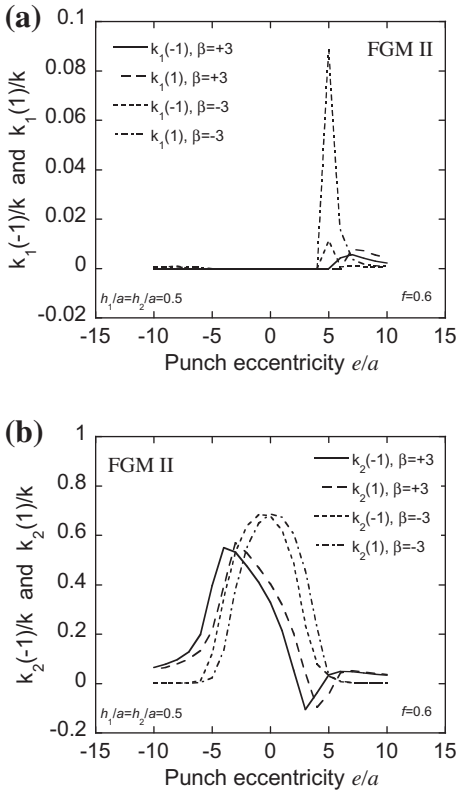

Fig. 8. Crack-closure computed Normalized mode I and II stress intensity factors $(k_1, k_2)/k$ variation with the punch eccentricity using the Orthotropic FGM II properties, for the case of a compliant coating $\beta a = -3$ and stiff coating $\beta a = 3$ and dry friction, $f = 0.6$; $k = p_0\sqrt{a}$, and for $\nu = 0.3$, $\delta = 4a, h_1 = h_2 = 0.5a$.

non-symmetric distribution is obtained with a stiff coating ($\beta a = +3$). Thus, we conclude that stiff coatings produce a reciprocating stress intensity factor which doubles the number of cycles to be counted for fatigue.

In Fig. 4, similar results are shown, but with friction coefficient $f = 0.6$, which corresponds to the case of dry friction. A conclusion similar to the previous case ($f = 0$) can be drawn. For mode II SIF $k_2(-1)$ and $k_2(+1)$, there is again a qualitative difference between the compliant case ($\beta a = -3$) and stiff cases ($\beta a = +3$). Compliant coating is more favorable. Our results are qualitatively similar to the results obtained by El-Borgi et al. (2004b) in the isotropic case. Quantitatively, numerical results show that –generally– with an orthotropic FGM, the peak of the SIFs is slightly lower than the peak of the SIFs with an isotropic FGM.

In both cases of Figs. 3 and 4, the mode I Stress Intensity Factor at one or both crack-tips becomes negative, which means that the crack faces are in contact over a certain part or over the entire crack length. The crack-closure algorithm developed by El-Borgi et al. (2004a) (described in Section 6), is applied to compute the correct stress intensity factors. The same algorithm computes the contact zone, and gives the abscises of the two tips of the crack.

Using the crack-closure algorithm, the SIFs in Fig. 5, are obtained. This case corresponds to the same one shown in Fig. 4, and illustrates the effect of the application of the crack-closure algorithm through the observation of the SIFs. The SIFs of the mode I are zero over a significant part of eccentricity values. The SIFs of the mode II, for the case of a compliant coating, $\beta a = -3$, have the same symmetric distribution but differ in their values from those shown in Fig. 4. In fact, their value was reduced by an order of magnitude of approximately 3 when the crack-closure algorithm is applied. Another result is that the sign of $k_2(-1)$ was inverted with the application of the crack-closure algorithm. However, the results obtained for the case of a stiff coating, $\beta a = +3$, have not the same anti-symmetric distribution as in Fig. 4, but they have the same order of magnitude.

Fig. 6 illustrates the crack length (position of left and right crack-tip) variation with the punch eccentricity, using the first kind of material properties (Orthotropic FGM I), for the case of dry friction and crack placed at mid-depth after applying a crack closure algorithm. The figure shows that for a compliant coating ($\beta a = -3$), the crack is closed over the part around zero of eccentricity values. While, for a stiff coating ($\beta a = -3$), the crack is closed over a significant part of eccentricity values. So, for a stiff coating the crack is more stable.

In Figs. 7 and 8, similar results, as the results given for FGM I in Figs. 4 and 5, are shown for FGM II, for the mode I and II SIFs: $k_1(-1)$, $k_1(+1)$, $k_2(-1)$ and $k_2(+1)$, when the friction coefficient is $f = 0.6$. Interpenetration of the crack surfaces has occurred (mode I SIFs have negative values). When crack-closure algorithm is applied; in the case of crack placed at mid-depth the mode I are zero over a significant part of eccentricity values. A comparison between Figs. 7,8 and Figs. 4,5 shows the effect of reinforced directions of the orthotropic FGM constituting the graded layer for, the normalized mode I and mode II normalized stress intensity factors. The stress intensity factors have the same distribution for the two kinds of FGM properties; however, their values are more important for the second kind of FGM properties than in the first kind. This result indicates that FGM II (where $c_{11} < c_{22}$) is more susceptible to cracking, thus using an FGM with properties similar to FGM I properties ($c_{11} > c_{22}$) is more efficient.

Figs. 9 and 10 show the effect of the thickness of the graded layer for, respectively, the normalized mode I and mode II stress intensity factors for the case of a compliant coating, $\beta a = -3$, and stiff coating, $\beta a = +3$. The crack is located at a constant depth

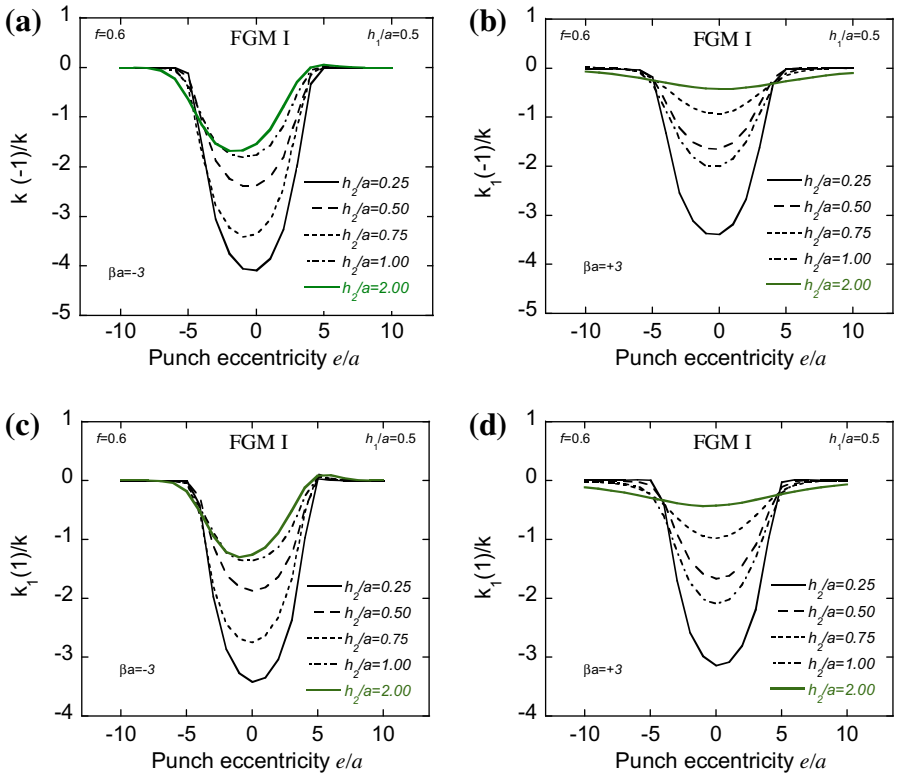

Fig. 9. Effect of FGM coating thickness on Normalized mode I stress intensity factor k_1/k variation with the punch eccentricity, using the first kind of material properties (FGM I), for the case of a compliant coating $\beta a = -3$ and a stiff coating $\beta a = 3$, and dry friction $f = 0.6$; disregarding crack-closure, $k = p_0\sqrt{a}$, and for $\nu = 0.3$, $\delta = 4a$, h_1 /a = 0.5 ; h_2 /a = 0.25, 0.5, 0.75, 1.0, 2.0 .

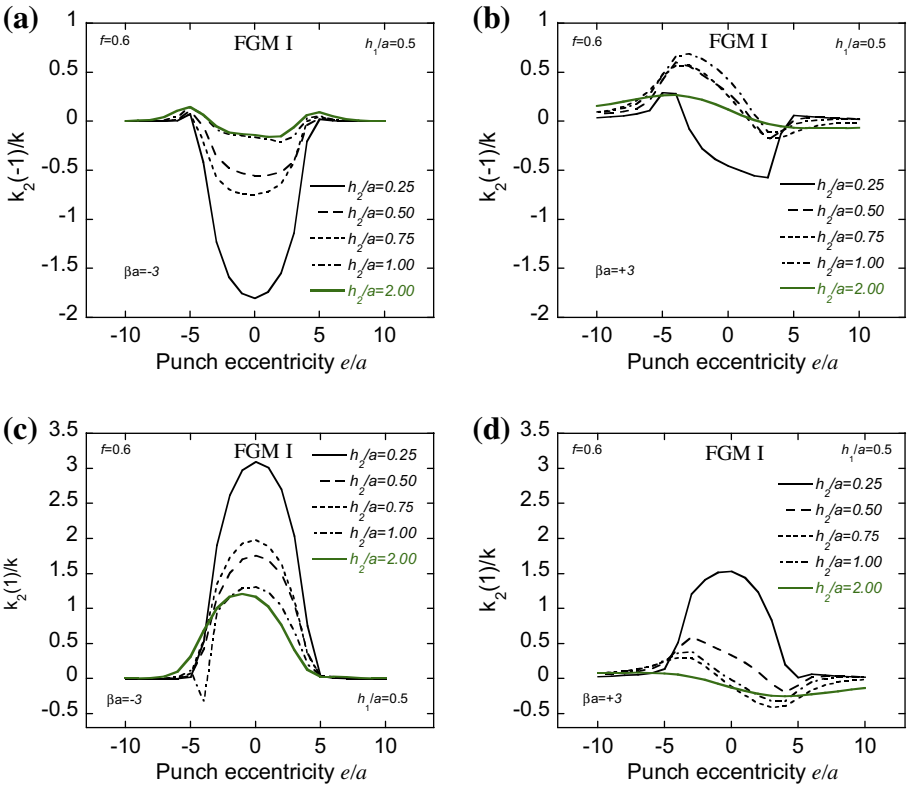

Fig. 10. Effect of FGM coating thickness on normalized mode II stress intensity factor k_2/k variation with the punch eccentricity, using the first kind of material properties (FGM I), for the case of a compliant coating $\beta a = -3$ and a stiff coating $\beta a = 3$, and dry friction $f = 0.6$; disregarding crack-closure, $k = p_0\sqrt{a}$, and for $\nu = 0.3$, $\delta = 4a$, h_1 /a = 0.5; h_2 /a = 0.25, 0.5, 0.75, 1.0, 2.0 .

$h_1 = 0.5a$ from the substrate. The thickness above the crack h_2 was varied from 0.25 a to 2a. As expected, the stress intensity factors are reduced when the thickness h_2 is increased while their distributions remain relatively similar.

8. Conclusion

In this paper, we considered an embedded crack in an orthotropic FGM layer bonded to a homogeneous semi-infinite medium, subject to statically applied normal and tangential surface loading. The crack is parallel to the free surface. Using integral transforms, the governing equations are converted into singular integral equations which are solved numerically to yield the displacement field as well as the crack-tip stress intensity factors. A detailed parametric study was conducted to investigate the effect of the material effects of the material orthotropy and non-homogeneity of the graded coating on the crack-tip stress intensity factors, using two different examples of orthotropic FGMs and different stiffness parameters. It can be concluded from this study that compliant coating is more favorable. In fact, stiff coating produces a reciprocating stress intensity factors which doubles the number of cycles to be counted for fatigue. We can also conclude that the grading direction of the orthotropic FGM layer has an effect on the stress intensity factors.

Appendix A. Solution of the uncracked medium

The solution of the uncracked composite medium (i.e. problem (1)) is briefly summarized in this appendix. To facilitate the solution, a new reference coordinate system $(x,\tilde{y})$ is assumed where $\tilde{y} = y + h_1$ as shown in Fig. 1. After applying the regularity conditions (Eqs. (13.a) and (13.b)), the solutions of the plane elasticity Eqs. (8.a)–(8.d) are given by:

$$u(x,\tilde{y}) = \int_{-\infty}^{+\infty} \left(\sum_{j=1}^{4} \tilde{C}_j(\alpha) e^{m_j \tilde{y}} \right) e^{-ix\alpha} d\alpha, \quad 0 < \tilde{y} < h, \tag{A.1}$$

$$v(x,\tilde{y}) = \int_{-\infty}^{+\infty} \left(\sum_{k=1}^{4} \tilde{C}_j(\alpha) s_j(\alpha) e^{m_j \tilde{y}} \right) e^{-ix\alpha} d\alpha, \quad 0 < \tilde{y} < h, \tag{A.2}$$

$$u(x,\tilde{y}) = \int_{-\infty}^{+\infty} \left(\tilde{C}_5(\alpha) + \tilde{C}_6(\alpha)\tilde{y} \right) e^{|\alpha|\tilde{y}} e^{-ix\alpha} d\alpha, \quad \tilde{y} \leqslant 0, \tag{A.3}$$

$$v(x,\tilde{y}) = \int_{-\infty}^{+\infty} \left[\tilde{C}_5(\alpha) s_5 + \tilde{C}_6(\alpha)(\tilde{y} s_5 + s_6) \right] e^{|\alpha|\tilde{y}} e^{-ix\alpha} d\alpha, \quad \tilde{y} \leqslant 0, \tag{A.4}$$

where h = h_1 + h_2 is the total thickness of the FGM layer, $m_j (j = 1,\ldots,4)$ are given by (24.a)–(24.d), and $s_j (j = 1,\ldots,6)$ are given by (26.a)–(26.c).

The unknown functions $\tilde{C}_j(\alpha)$ (j = 1 … 6) are determined from the boundary conditions ((9.a)–(12.b)) which are rewritten in the new coordinate system $(x,\tilde{y})$ as follows:

$$\sigma_{xy}(x,h) = p_t(x), \quad |x-e| \leqslant \delta, \tag{A.5.a}$$

$$\sigma_{xy}(x,h) = 0, \quad |x-e| > \delta, \tag{A.5.b}$$

$$\sigma_{yy}(x,h) = -p_n(x), \quad |x-e| \leqslant \delta, \tag{A.6.a}$$

$$\sigma_{yy}(x,h) = 0, \quad |x-e| > \delta, \tag{A.6.b}$$

$$\sigma_{xy}(x,0^+) = \sigma_{xy}(x,0^-), \quad |x| < +\infty, \tag{A.7.a}$$

$$\sigma_{yy}(x,0^+) = \sigma_{yy}(x,0^-), \quad |x| < +\infty, \tag{A.7.b}$$

$$u(x,0^+) = u(x,0^-), \quad |x| < +\infty. \tag{A.8.a}$$

$$v(x,0^+) = v(x,0^-), \quad |x| < +\infty. \tag{A.8.b}$$

The application of the boundary conditions (A.5.a)–(A.8.b) leads to a linear algebraic system of equations for the unknowns functions $\tilde{C}_j(\alpha)(j = 1\ldots6)$:

$$\begin{bmatrix} \tilde{q}_1 e^{m_1 h} & \tilde{q}_2 e^{m_2 h} & \tilde{q}_3 e^{m_3 h} & \tilde{q}_4 e^{m_4 h} & 0 & 0 \\ \tilde{p}_1 e^{m_1 h} & \tilde{p}_2 e^{m_2 h} & \tilde{p}_3 e^{m_3 h} & \tilde{p}_4 e^{m_4 h} & 0 & 0 \\ \tilde{q}_1 & \tilde{q}_2 & \tilde{q}_3 & \tilde{q}_4 & -\tilde{q}_5 & -\tilde{q}_6 \\ \tilde{p}_1 & \tilde{p}_2 & \tilde{p}_3 & \tilde{p}_4 & -\tilde{p}_5 & -\tilde{p}_6 \\ 1 & 1 & 1 & 1 & -1 & 0 \\ s_1 & s_2 & s_3 & s_4 & -s_5 & -s_6 \end{bmatrix} \begin{Bmatrix} \tilde{C}_1 \\ \tilde{C}_2 \\ \tilde{C}_3 \\ \tilde{C}_4 \\ \tilde{C}_5 \\ \tilde{C}_6 \end{Bmatrix} = \begin{Bmatrix} \tilde{Q} \\ \tilde{P} \\ 0 \\ 0 \\ 0 \\ 0 \end{Bmatrix} \tag{A.9}$$

In which:

$$\tilde{Q}(\alpha) = \frac{1}{c_{660}} \frac{e^{-\beta h_2}}{2\pi} \int_{e-\delta}^{e+\delta} p_t(x) e^{i\alpha x} dx, \tag{A.10.a}$$

$$\tilde{P}(\alpha) = -\frac{(\kappa-1)}{c_{660}} \frac{e^{-\beta h_2}}{2\pi} \int_{e-\delta}^{e+\delta} p_n(x) e^{i\alpha x} dx, \tag{A.10.b}$$

$$\tilde{q}_j = m_j - i\alpha s_j, \quad (j = 1,\ldots,4),$$

$$\tilde{q}_5 = \frac{\mu}{c_{660}}(|\alpha| - i\alpha s_5) = 2|\alpha| \frac{\mu}{c_{660}}, \tag{A.11.a-f}$$

$$\tilde{q}_6 = -\frac{\mu}{c_{660}}(i\alpha s_6 - 1) = \frac{\mu}{c_{660}}(1-\kappa),$$

$$\tilde{p}_j = \frac{\kappa-1}{c_{660}}(c_{220} m_j s_j - i c_{120}\alpha), \quad (j = 1,\ldots,4),$$

$$\tilde{p}_5 = \frac{\mu}{c_{660}}((1+\kappa)s_5|\alpha| - i(3-\kappa)\alpha) = 2i\frac{\mu}{c_{660}}\alpha(\kappa-1), \tag{A.12.a-f}$$

$$\tilde{p}_6 = \frac{\mu}{c_{660}}(1+\kappa)(|\alpha| s_6 + s_5) = i\frac{\mu}{c_{660}}\frac{\alpha}{|\alpha|}(1-\kappa^2),$$

The system of equations (A.9) can be inverted analytically as follows:

$$\tilde{C}_k = (-1)^{k+1} \frac{\tilde{D}_{1k}}{\tilde{D}} \tilde{Q}(\alpha) + (-1)^k \frac{\tilde{D}_{2k}}{\tilde{D}} \tilde{P}(\alpha), \tag{13}$$

in which $\tilde{D}$ is the determinant and $\tilde{D}_{ij}(i,j = 1,\ldots,6)$ is the subdeterminant of the matrix in (A.9) corresponding to the elimination of the ith row and jth column.

The solution of the problem can be written as:

$$\sigma_{xy} = e^{\beta(\tilde{y}-h_1)} \int_{-\infty}^{+\infty} \sum_{j=1}^{4} \tilde{q}_j \tilde{C}_j e^{m_j \tilde{y}} e^{-ix\alpha} d\alpha, \text{ and } \sigma_{yy} = \frac{e^{\beta(\tilde{y}-h_1)}}{(\kappa-1)} \int_{-\infty}^{+\infty} \sum_{j=1}^{4} \tilde{p}_j \tilde{C}_j e^{m_j \tilde{y}} e^{-ix\alpha} d\alpha \tag{14}$$

By substituting the constants $\tilde{C}_k(\alpha)(k = 1,\ldots,6)$ by their determined values, the solution of the uncracked problem is:

$$\sigma_{xy} = \frac{e^{\beta(\tilde{y}-h_1)}}{2\pi} \int_{e-\delta}^{e+\delta} \int_{-\infty}^{+\infty} \left(\sum_{k=1}^{4} (-1)^{k+1} \frac{\tilde{D}_{1k}}{\tilde{D}} \tilde{q}_j e^{m_j \tilde{y}} \right) p_t(t) e^{i\alpha(t-x)} d\alpha dt - \frac{e^{\beta(\tilde{y}-h_1)}}{2\pi} \int_{e-\delta}^{e+\delta} \int_{-\infty}^{+\infty} \left(\sum_{k=1}^{4} (-1)^k \frac{\tilde{D}_{2k}}{\tilde{D}} \tilde{q}_j e^{m_j \tilde{y}} \right) (\kappa-1) p_n(t) e^{i\alpha(t-x)} d\alpha dt \tag{A.14.a}$$

$$\sigma_{yy} = \frac{e^{\beta(\tilde{y}-h_1)}}{2\pi(\kappa-1)} \int_{e-\delta}^{e+\delta} \times \int_{-\infty}^{+\infty} \left(\sum_{j=1}^{4} (-1)^{k+1} \frac{\tilde{D}_{1k}}{\tilde{D}} \tilde{p}_j e^{m_j \tilde{y}} \right) p_t(t) e^{i\alpha(t-x)} d\alpha dt - \frac{e^{\beta(\tilde{y}-h_1)}}{2\pi} \int_{e-\delta}^{e+\delta} \times \int_{-\infty}^{+\infty} \left(\sum_{j=1}^{4} (-1)^{k} \frac{\tilde{D}_{2k}}{\tilde{D}} \tilde{p}_j e^{m_j \tilde{y}} \right) p_n(t) e^{i\alpha(t-x)} d\alpha dt \quad \text{(A.14.b)}$$

Appendix B

B1. Expressions of quantities appearing in (29):

$$q_j = m_j - i\alpha s_j \quad (j = 1, \ldots, 4),$$

$$q_5 = \frac{\mu}{c_{660}} (|\alpha| - i\alpha s_5), \quad \text{(B.1.a-f)}$$

$$q_6 = -\frac{\mu}{c_{660}} (|\alpha| h_1 + i\alpha(s_6 - s_5 h_1) - 1),$$

$$p_j = \frac{\kappa - 1}{c_{660}} (c_{220} m_j s_j - i c_{120} \alpha) \quad (j = 1, \ldots, 4),$$

$$p_5 = \frac{\mu}{c_{660}} ((1+\kappa) s_5 |\alpha| - i(3-\kappa)\alpha), \quad \text{(B.2.a-f)}$$

$$p_6 = \frac{\mu}{c_{660}} ((1+\kappa)[|\alpha|(s_6 - s_5 h_1) + s_5] + i(3-\kappa)\alpha h_1)$$

where m_j (j = 1,. . ., 4) and s_j (j = 1,. . ., 6) are, respectively, given by (24) and (26).

B2. Expressions of quantities appearing in (31): Fredholm Kernels

The Fredholm kernels, used in writing the integral equations are given by the following expressions:

$$k_{11}(x,t) = \lim_{y \to 0^-} \int_0^{+\infty} \left(\frac{\sqrt{\kappa_0 + \sqrt{\delta_0}}}{\sqrt{2}(\kappa_0 + \upsilon_0)} N_{11}(\alpha, y) - 1 \right) \sin(\alpha(t-x)) d\alpha, \quad \text{(B.3.a)}$$

$$k_{12}(x,t) = \lim_{y \to 0^-} \int_0^{+\infty} \times \frac{\sqrt{\kappa_0 + \sqrt{\delta_0}}}{\sqrt{2}(\kappa_0 + \upsilon_0)} N_{12}(\alpha, y) \cos(\alpha(t-x)) d\alpha, \quad \text{(B.3.b)}$$

$$k_{21}(x,t) = \lim_{y \to 0^-} \int_0^{+\infty} \times \frac{\sqrt{\delta_0}\sqrt{\kappa_0 + \sqrt{\delta_0}}}{\sqrt{2}(\kappa - 1)(\kappa_0 + \upsilon_0)} N_{21}(\alpha, y) \cos(\alpha(t-x)) d\alpha, \quad \text{(B.3.c)}$$

$$k_{22}(x,t) = \lim_{y \to 0^-} \int_0^{+\infty} \left(\frac{\sqrt{\delta_0}\sqrt{\kappa_0 + \sqrt{\delta_0}}}{\sqrt{2}(\kappa - 1)(\kappa_0 + \upsilon_0)} N_{22}(\alpha, y) - 1 \right) \sin(\alpha(t-x)) d\alpha, \quad \text{(B.3.d)}$$

where

$$N_{11}(\alpha, y) = -\frac{2}{\alpha} \sum_{j=1}^{4} (-1)^{j+13} \frac{D_{j+4}^{9}}{D} q_j e^{m_j y}, \quad \text{(B.4.a)}$$

$$N_{12}(\alpha, y) = \frac{2i}{\alpha} \sum_{j=1}^{4} (-1)^{j+14} \frac{D_{j+4}^{10}}{D} q_j e^{m_j y}, \quad \text{(B.4.b)}$$

$$N_{21}(\alpha, y) = \frac{2i}{\alpha} \sum_{j=1}^{4} (-1)^{j+13} \frac{D_{j+4}^{9}}{D} p_j e^{m_j y}, \quad \text{(B.4.c)}$$

$$N_{22}(\alpha, y) = -\frac{2}{\alpha} \sum_{j=1}^{4} (-1)^{j+14} \frac{D_{j+4}^{10}}{D} p_j e^{m_j y}, \quad \text{(B.4.d)}$$

in which D is the determinant of the matrix corresponding to the linear algebraic system and D_j^i is its sub-determinant corresponding to the elimination of the ith row and jth column.

References

Aoulou, W., Yildirim, B., El-Borgi, S., Zghal, A., 2009. Buckling of an orthotropic graded coating with an embedded crack bonded to a homogeneous substrate. International Journal of Solids and Structures 46, 1890–1900.

Chen, Y.F., Erdogan, F., 1996. The interface crack problem for a nonhomogeneous coating bonded to a homogeneous substrate. Journal of Mechanics and Physics of Solids 44, 771–787.

Chen, J., Liu, Z., Zou, Z., 2002. Transient internal crack problem for a nonhomogeneous orthotropic strip (Mode I). International Journal of Engineering Science 40, 1761–1774.

Choi, H.J., 2004. Impact response of a surface crack in a coating/substrate system with a functionally graded interlayer: antiplane deformation. International Journal of Solids and Structures 41, 5631–5645.

Dag, S., 2001. Crack and contact problem in graded materials. PhD Dissertation, Lehigh University Bethlehem, Pennsylvania, USA.

Dag, S., Erdogan, F., 2002. A surface crack in a graded medium under general loading condition. ASME Journal of Applied Mechanics 69, 580–588.

Dag, S., Ilhan, K.A., 2008. Mixed-mode fracture analysis of orthotropic functionally graded material coatings using analytical and computational methods. Journal of Applied Mechanics 75, 051104-9.

Dag, S., Kadioglu, S., Yahsi, O.S., 1999. Circumferential crack problem for an FGM cylinder under thermal stresses. Journal of Thermal Stresses 22, 659–687.

Dag, S., Yildirim, B., Sarikaya, D., 2007. Mixed-mode fracture analysis of orthotropic functionally graded materials under mechanical and thermal loads. International Journal of Solids and Structures 44, 7816–7840.

Delale, F., Erdogan, F., 1983. The crack problem for a nonhomogeneous plane. ASME Journal of Applied Mechanics 50, 609–614.

Dhaliwal, R.S., Singh, B.M., 1978. On the theory of elasticity of a non-homogeneous medium. Journal of Elasticity 8, 211–219.

Eberhardt, A.W., Kim, B.S., 1998. Stress intensity factors for a vertical surface crack in polyethylene subject to rolling and sliding contact. ASME Journal of Biomechanical Engineering 120, 778–783.

El-Borgi, S., Erdogan, F., Ben Hatira, F., 2003. Stress intensity factors for an interface crack between a functionally graded coating and a homogeneous substrate. International Journal of Fracture 123, 139–162.

El-Borgi, S., Erdogan, F., Hidri, L., 2004a. A partially insulated embedded crack in an infinite functionally graded medium under thermo-mechanical loading. International Journal of Engineering Science 42, 371–393.

El-Borgi, S., Keer, L., Ben Said, W., 2004b. An embedded crack in a functionally graded coating bonded to a homogeneous substrate under frictional Hertzian contact. Wear 257 (7–8), 760–776.

Erdogan, F., 1985. The crack problem for bonded nonhomogeneous materials under antiplane shear loading. ASME Journal of Applied Mechanics 52, 823–828.

Erdogan, F., 1995. Fracture mechanics of functionally graded materials. Composites Engineering 5, 753–770.

Erdogan, F., Gupta, G.D., Cook, T.S., 1973. Numerical solution of singular integral equations. In: Sih, G.C. (Ed.), Mechanics of Fracture. Norrdhoff, Leyden, pp. 368–425.

Erdogan, F., Wu, B.H., 1996. Crack problems in FGM layers under thermal stresses. Journal of Thermal Stresses 19, 237–265.

Erdogan, F., Wu, B.H., 1997. The surface crack problem for a plate with functionally graded properties. ASME Journal of Applied Mechanics 64, 449–456.

Feng, W.J., Zhang, Z.G., Zou, Z.Z., 2003. Impact failure prediction of mode III crack in orthotropic functionally graded strip. Theoretical and Applied Fracture Mechanics 40, 97–104.

Gharbi, M., El-Borgi, S., Chafra, M., 2009. A surface crack in a graded coating bonded to a homogeneous substrate under transient thermal loading. Journal of Thermal Stresses 32 (4), 394–413.

Gharbi, M., El-Borgi, S., Chafra, M., 2011. A surface crack in a graded coating bonded to a homogeneous substrate under dynamic loading conditions. International Journal of Engineering Science 49, 677–693.

Guo, L.-C., Wu, L.-Z., Zeng, T., Ma, L., 2004. Mode I crack problem for a functionally graded orthotropic strip. European Journal of Mechanics A/Solids 23, 219–234.

Holt, J., Koizumi, M., Hirai, T., Munir, Z.A. (Eds.), 1992. Functionally gradient materials. Ceramic Transactions, vol. 34. The American Ceramic Society, Ohio.

Jin, Z.-H., Noda, N., 1993. An internal crack parallel to the boundary of a nonhomogeneous half plane under thermal loading. International Journal of Engineering Science 31, 793–806.

Jin, Z.-H., Noda, N., 1994. Crack-tip singular fields in nonhomogeneous materials. ASME Journal of Applied Mechanics 61, 738–740.

Kadioglu, S., Dag, S., Yahsi, S., 1998. Crack problem for a functionally graded layer on an elastic foundation. International Journal of Fracture 94, 63–77.

Kayserr, W.A., Ilsscner, B., 1995. FGM research activities in Europe. MRS Bulletin 20, 22–26.

Kim, J.-H., KC, A., 2008. A generalized interaction integral method for the evaluation of the T-stress in orthotropic functionally graded materials under thermal loading. Journal of Applied Mechanics 75 (5), 051112-11.
Kim, J.-H., Paulino, G.H., 2002. Mixed-mode fracture of orthotropic functionally graded materials using finite elements and the modified crack closure method. Engineering Fracture Mechanics 69, 1557–1586.
Kim, J.-H., Paulino, G.H., 2003. Mixed-mode J-integral formulation and implementation using graded elements for fracture analysis of nonhomogeneous orthotropic materials. Mechanics of Materials 35, 107–128.
Kim, J.-H., Paulino, G.H., 2004. The interaction integral for fracture of orthotropic graded materials: evaluation of stress intensity factors. International Journal of Solids and Structures 40, 3967–4001.
Konda, N., Erdogan, F., 1994. Mixed mode crack problem in a non-homogeneous elastic medium. Engineering Fracture Mechanics 47, 533–547.
Lee, Y.D., Erdogan, F., 1998. Interface cracking of FGM coatings under steady state heat flow. Engineering Fracture Mechanics 59, 361–380.
Li, X.F., Guo, S.H., 2006. Effects of nonhomogeneity on dynamic stress intensity factors for an antiplane interface crack in a functionally graded material bonded to an elastic semi-strip. Computational Materials Science 38, 432–441.
Li, X.F., Fan, T.Y., 2007. Dynamic analysis of a crack in a functionally graded material sandwiched between two elastic layers under anti-plane loading. Composite Structures 79, 211–219.
Liu, C.H., Chen, I.F., 1996. Interface cracks in a layered solid subjected to contact stresses. ASME Journal of Applied Mechanics 63, 271–277.
Noda, N., Jin, Z.-H., 1993. Steady thermal stresses in an infinite nonhomogeneous elastic solid containing a crack. Journal of Thermal Stresses 16, 181–196.
Oliveira, S., Bower, A.F., 1996. An analysis of fracture and delamination in thin coatings subjected to contact loading. Wear 198, 15–32.
Ozturk, M., Erdogan, F., 1993. The axisymmetric crack problem in a nonhomogeneous medium. ASME Journal of Applied Mechanics 44, 631–636.
Ozturk, M., Erdogan, F., 1997. Mode I crack problem in an inhomogeneous orthotropic medium. International Journal of Engineering Science 35, 869–883.
Ozturk, M., Erdogan, F., 1999. The mixed mode crack problem in an inhomogeneous orthotropic medium. International Journal of Fracture 98, 243–261.
Sampath, S., Herman, H., Shimoda, N., Saito, T., 1995. Thermal spray processing of FGMs. MRS Bulletin 20, 27–31.
Suresh, S., Giannakopoulos, A.-E., Alcala, J., 1997. Spherical indentation of compositionally graded materials: theory and experiments. Acta Materialia 45, 1307–1321.
Zhou, Y., Li, X., Qin, J.Q., 2007. Transient thermal stress analysis of orthotropic functionally graded materials with a crack. Journal of Thermal Stresses 30, 1211–1231.
Zhou, Y., Li, X., Yu, D., 2009. Transient thermal response of a partially insulated crack in an orthotropic functionally graded strip under convective heat supply. CMES 43 (3), 191–221.
Zhou, Y., Li, X., Yu, D., 2010. A partially insulated interface crack between a graded orthotropic coating and a homogeneous orthotropic substrate under heat flux supply. International Journal of Solids and Structures 47, 768–778.